Hindawi
Journal of Advanced Transportation
Volume 2023, Article ID 3964616, 14 pages
https://doi.org/10.1155/2023/3964616

Research Article

A Signal Optimization Model of Adjacent Closely Spaced Intersections Which Optimizes Pedestrian Crossing

Jiawen Wang[1], **Hao Chen**[1], **Jiayu Hang**[2], **Mingjie Xu**[3] **and Yin Han**[1]

[1]*Business School, University of Shanghai for Science and Technology, Shanghai 200093, China*
[2]*School of Urban Rail Transportation, Changzhou University, Jiangsu, Changzhou 213164, China*
[3]*Shanghai K&Z Construction Project Management Co., Ltd., Shanghai 201616, China*

Correspondence should be addressed to Yin Han; hanyin2000@126.com

Received 19 October 2022; Revised 19 November 2022; Accepted 5 April 2023; Published 10 May 2023

Academic Editor: Avinash Unnikrishnan

Adjacent closely spaced intersections with characteristics of short link distance and high pedestrian flow are primarily located in high-density urban areas. To address the problems of queue overflow, poor traffic operation, and high pedestrian travel delays, a pedestrian-motor vehicle signal optimization method for adjacent closely spaced intersections was proposed in this paper. First, the traffic flow entering the closely spaced intersections is divided into nonarterial and arterial flow categories to establish a delay model of pedestrian crossing. Then, a pedestrian crossing delay model based on pedestrian demand is constructed according to pedestrian crossing time and a space diagram. An optimization model for pedestrians and vehicles at adjacent closely spaced intersections is established, and an artificial intelligence algorithm is used to optimize this model. Finally, a selected case intersection is optimized. The results show that compared with a traditional single optimization method, vehicle delay decreased about 4%, 13.8%, 17.1%, and 25.9% and total pedestrian delay decreased by 3%, 15%, 25%, and 31%, respectively, for the four proposed scenarios.

1. Introduction

As the social economy expands and the land use of urban areas increases, supporting facilities, such as road resources, must be constantly improved. With the accompanying land development and road construction, a greater demand is made for land use [1]. As a result, many new roads have been built, leading to an increase in the number of intersections, which formed the adjacent closely spaced intersections. The spacing between adjacent intersections becomes increasingly shorter, which results in a smaller link capacity [2]. A slight fluctuation and overflow of traffic flow will lead to disorder at intersections [3]. Compared with traditional adjacent intersections, adjacent closely spaced intersections are more affected by the fluctuation of traffic flow [4]. The situation of vehicles yielding to pedestrians also seriously degrades the operating efficiency of the intersection [5]. To reduce the travel delays of vehicles and pedestrians, it is needed to study and improve the operation efficiency of adjacent closely spaced intersections. The intersection optimization methods are concentrated on two specific aspects. The first is to improve the physical characteristics of the intersections. By the construction of underground passages and erection of viaducts and bridges, it is possible to isolate the conflict and shunt the traffic flow. This process requires a significant workforce, material, and financial resources, which will pollute the environment with construction noise, exhaust gas, and waste. The second uses the angle of signal control. Reasonable signals are utilized to optimize the intersections for both vehicles and pedestrians [6].

A lot of research has been accumulated on the optimization of vehicle and pedestrian signals. Some scholars focus on pedestrian crossing safety and study the mechanism of pedestrian crossing [7, 8]. Other scholars focus on traffic efficiency and optimize signal timing at signalized intersections by taking efficiency indicators such as delay and traffic capacity as optimization objectives [9–11]. However, most of these studies have focused on isolated intersections.

Although some studies have designed midblock crosswalks between adjacent intersections, it has been proven that it only slightly impacts vehicles [12]. However, few studies have focused on considering the efficiency of vehicles and pedestrians at traditional adjacent intersections, especially at adjacent closely spaced intersections.

On the basis of the existing research, this paper first analysed the operation mechanism of vehicles at adjacent closely spaced intersections. Secondly, considering the influence of pedestrians, the signal set of the downstream intersection is adjusted according to the traffic arrival condition of the upstream intersection. This paper is divided into four scenarios, which are the vehicle platoons reaching downstream at the initial red phase, the middle of the red phase, the initial green phase, and the middle of the green phase. Then, the delay models of the four scenarios are connected by the weight coefficients to obtain the optimal timing model for pedestrians and vehicles. Finally, the genetic algorithm is used to solve the model.

The contributions of this paper are as follows.

(a) The traffic flow entering the closely spaced intersections is divided into nonarterial and arterial flow categories to establish a delay model of pedestrian crossing. Based on the arrival of the arterial traffic at downstream intersections, discrete platoon arrival delay models considering pedestrians are developed.

(b) An integrated optimization method is proposed to optimize delay for pedestrians and vehicles, and this method reduces the total intersection approach vehicle delay level by 4%–25.9% and the total pedestrian delay by 3%–31% compared with the isolated intersection optimizing method.

2. Literature Review

For the study of adjacent intersections, many scholars have studied and proposed various models and intelligent control algorithms to reduce traffic delays. Xinwu et al. proposed a coordinated control method of main signals at adjacent closely spaced intersections based on an improved genetic algorithm [13]. Gu and Shao used the characteristics of saturated traffic flow on urban roads in China to establish a model for the optimization of phase offset for adjacent interactions. The genetic algorithm was used to solve the problem and improve the traffic efficiency of the intersection [14]. Zou et al. searched for the optimal phase of the adjacent intersections. The transition probabilities of the connection lanes of intersections 1 and 2 are introduced, which are utilized to compute the arrival rates of the connection lanes, and a corresponding model of the phases of the connection lanes is proposed [15]. Zhang et al. propose a coordinated control model based on the platform to optimize the offset between adjacent intersections. Genetic algorithm is executed to solve the model. The performance evaluations show that the model not only effectively reduces average delay on arterial roads but also lowers the sensitivity of signal control for flow fluctuations [16].

It can be found from the review that the current research on the signal control of adjacent intersections rarely considers the need for pedestrian crossing. In addition, the adjacent closely spaced intersections are rarely focused. Research on pedestrian signal control strategy mainly focuses on the leading pedestrian intervals (LPI) and the exclusive pedestrian phase (EPP) and mainly consider the impact of safety and efficiency for separate optimization. The leading pedestrian intervals (LPI) refer to that when pedestrians and vehicles cross the street in the same direction; the pedestrian green signal will light up a few seconds in advance. The setting of LPI can not only improve pedestrian safety but also have little impact on vehicles. When LPI is set to 3 s, it can effectively reduce the conflict between people and vehicles [17]. Goughnour et al. developed crash correction coefficients primarily for improving left-turn phasing and LPI and showed that LPI significantly reduced vehicle-pedestrian collisions [18]. Furth and Saeidi Razavi developed models to estimate the loss of capacity due to LPI and LTI (leading through intervals) in a range of scenarios [19]. Saneinejad and Lo provided a guide for implementation and evaluation that can determine a reasonable location and duration of LPI [20].

The exclusive pedestrian phase (EPP) refers to providing a dedicated phase for pedestrians. During this phase, pedestrians can pass in all directions and vehicles cannot pass. When the dedicated phase time of pedestrians is too long, more people will cross the street illegally [21]. When the pedestrian violation rate is low, the setting of EPP will have a more obvious effect [22]. The setting of EPP reduces the incidence of pedestrian-vehicle conflict by 7%–63% and reduced the pedestrian crossing distance by 13%, but it did not improve the traffic efficiency of pedestrians and vehicles [23]. Wang et al. analysed the effectiveness of setting EPP under different vehicle yield rates considering the impact of human-vehicle interaction [24]. Juozevičiūtė and Grigonis studied the effectiveness of EPP signalized intersections in vehicle-pedestrian collisions, resulting in pedestrian injury or death and showed that pedestrian accidents can be reduced by up to 100% [25].

It can be found from the review that the current research on pedestrian signal control strategies mainly focuses on individual optimization, lacking a unified time phase optimizing framework. Based on previous studies, the optimal delay model of pedestrian and vehicle is established in this paper in order to improve the traffic efficiency.

3. Methodology

3.1. Problem Description. There are four intersections, A, B, C and D, in Figure 1, where A and B are closely spaced intersections. Overflows can occur with slight fluctuations in traffic flow at adjacent closely spaced intersections. The overflow at the intersection A and B affected the surrounding intersections C and D. This paper will optimize the signal timing of the adjacent closely spaced intersections under the consideration of the pedestrian crossing demand to avoid this situation.

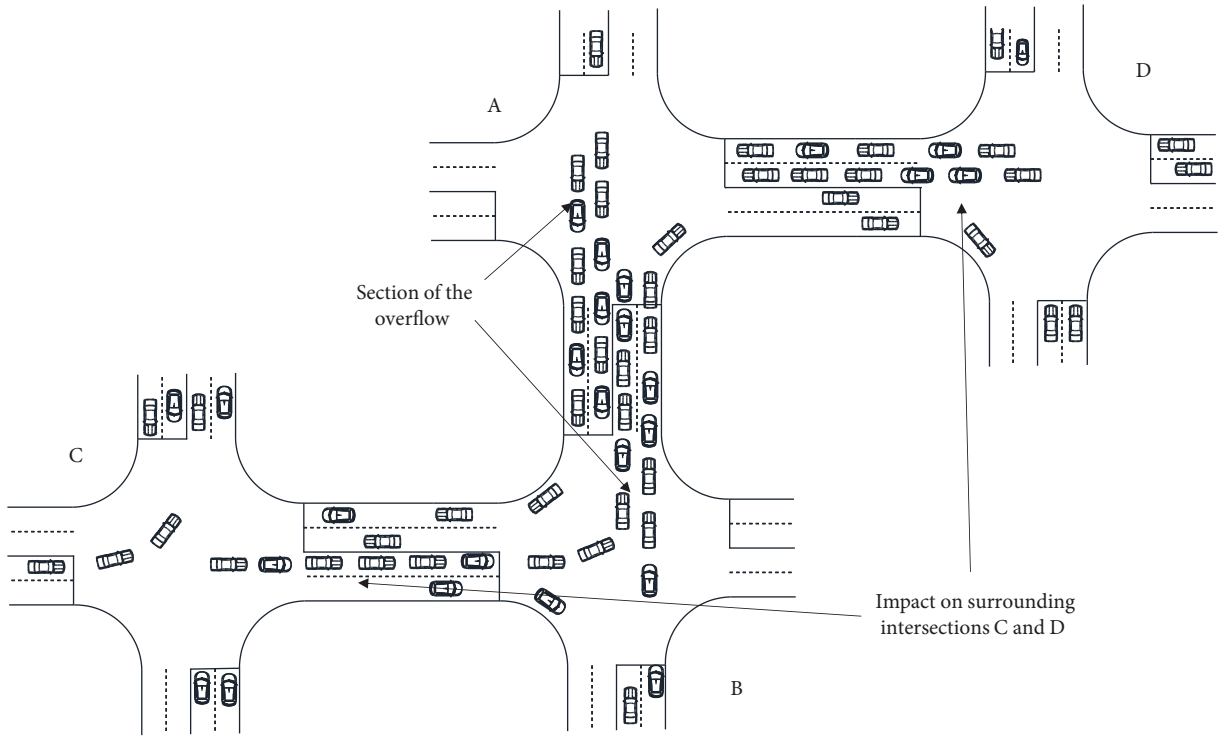

Figure 1: Diagram of the problem.

3.2. Operational Hypothesis. The actual headway data are utilized to verify the departure road's headway distribution. The fitted data are shown in Table 1. The headway distribution was assumed to follow the Poisson distribution, and the chi-square test was used to prove the hypothesis. The significance level α is equal to 0.05. The chi-square value χ^2 was calculated to be 10.78. According to the chi-square critical value table, the corresponding chi-square critical value is 11.070 larger than the chi-square value χ^2. It is verified that the hypothesis is acceptable. Hence, in this paper, the headway distribution on the departure road at the intersection is assumed to obey Poisson distribution.

The following assumptions are proposed for an optimal control system:

(a) All drivers and pedestrians abide by traffic rules and behave legally. Pedestrians can quickly respond to the vehicle's behaviour (quick crossing) and the interaction between pedestrians is ignored.

(b) The arrival time of pedestrians at the intersection obeys Poisson distribution and remains stable in a period.

(c) The arrival time of vehicle in closely spaced intersections obeys Poisson distribution.

3.3. The Operation Mechanism of Vehicles at Adjacent Closely Spaced Intersections. Through the analysis of specific traffic flow conditions, when vehicles enter into closely spaced intersections, the way of vehicles exiting can be divided into two situations: (i) not passing through the merging route and directly exit the short-distance intersection system; (ii) first, it merges into the arterial road merging path shown in Figure 2, passes through the downstream intersections, and finally exits the entire short-distance intersection system. It consists of traffic flow on the arterial road through straight traffic and the left-turning and right-turning traffic on the branch roads.

Table 1: Vehicles leaving the departure road.

Time headway (s)	Frequency of cumulative observation	Frequency of theoretical observation
(0, 3]	70	71.4015
(3, 6]	62	50.1202
(6, 9]	28	31.3240
(9, 12]	13	19.5570
(12, 15]	6	12.2385
(15, 18]	8	7.6465
>18	18	12.7305

In this paper, traffic flow that directly leaves the closely spaced intersection is called nonarterial traffic flow and those passing through the junction and diversion points are called arterial traffic flows. The delay of the closely spaced intersection system should be the sum of the delay with nonarterial flow and arterial traffic. The delay of nonarterial flow belongs to isolated intersection delays using the HCM2010 delay model to calculate. The arterial traffic flow is more complicated. After gathering again, it is subject to the delay caused by the signal control of the downstream intersection.

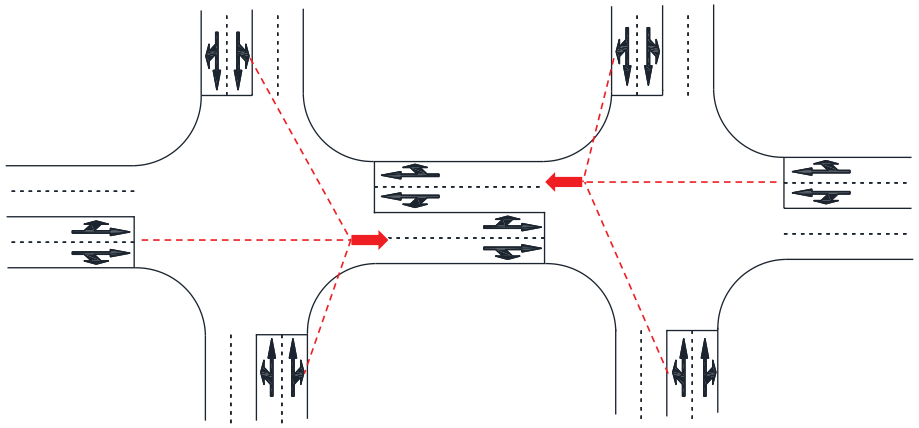

Figure 2: Schematic diagram of motor vehicle operation.

It is worth noting that the traffic flow from the upstream intersection often arrives at the downstream intersection in the form of a vehicle platoon. The time when the vehicle platoon arrives at the downstream intersection is different. Therefore, the delay is different. The vehicle platoon, which comes downstream, is considered specifically to improve the accuracy of model [26]. When the vehicle platoon reaches the downstream intersection, four scenarios may encounter: (i) initial stage of red light, (ii) middle stage of red light, (iii) initial stage of green light, and (iv) middle stage of green light. In this study, the delay models of four scenarios are integrated into the arterial road traffic delay model by setting the dynamic weight coefficient.

3.4. Traffic Delay Model. In this section, the vehicle delay model for adjacent closely spaced intersections was established, and then a pedestrian delay model was proposed.

The description of parameters in this paper is shown in Table 2.

3.4.1. Nonarterial Road Traffic Delay Model. The nonarterial road traffic delay is derived by the following method:

$$d_{ij}^{v} = \frac{0.5C\left(1-\left(g_i/c\right)\right)^2}{1-\left[\min\left(1,X\right)\left(g_i/c\right)\right]} + 900T\left[\left(X-1\right)+\sqrt{\left(X-1\right)^2+\frac{8KIX}{QT}}\right]. \tag{1}$$

The total delay of nonarterial road traffic was calculated as follows:

$$d_{\mathrm{v}}^{1} = \sum_{i}\sum_{j} d_{ij}^{\mathrm{v}} q_{ij}^{\mathrm{v}}. \tag{2}$$

3.4.2. Arterial Road Traffic Delay Model. As shown in Figure 3, the vehicle platoon arrives at the downstream intersection at the red phase. The accumulation of vehicles without pedestrian interference is shown in Figure 3(a). Within a few seconds, after the vehicle obtains the right of way, the crosswalk is still in the late discrete state, and the delay under the influence of pedestrians is shown in Figure 3(b). The shaded area represents the vehicle delay in this scenario. The corresponding calculation is as follows:

$$\begin{aligned} d_{\mathrm{e}}^{1} &= \int_{0}^{r}\left[\left(q_2+2q_3+s\right)t+2\left(q_2-q_3\right)t_{\mathrm{c}}^{1}-sr\right]\mathrm{d}t, \\ \ddot{d}_{\mathrm{e}}^{1} &= d_{e}^{1}+\int_{r}^{r+\Delta t_1+\ddot{t}_{\mathrm{e}}^{1}}\left[\left(q_3+s\right)t+\left(q_2-q_3\right)t_{\mathrm{c}}^{1}-sr\right]\mathrm{d}t-\ddot{t}_{\mathrm{e}}^{1}\left(\ddot{t}_{\mathrm{e}}^{1}+r+\Delta t_1\right)0.5\overline{q}. \end{aligned} \tag{3}$$

Figure 4 shows a platoon arriving at the downstream intersection in the middle of a red phase. Figure 4(a) shows the cumulation of vehicles without pedestrian interference. Figure 4(b) shows the cumulation of vehicles with the interference of pedestrians. Delay is in the shaded area of Figures 4(a) and 4(b). The formulas of vehicles delay are

Table 2: Parameters' description.

Parameters	Description	Unit
Decision variable		
C	Cycle length	s
g	Effective green time	s
g_p	Effective green time for pedestrians	s
r	Red light time	s
Input parameter		
q_{ij}^v	Volume of intersection entrance lane j under phase i	veh/h
Q	Intersection capacity	veh/h
q_1	Flow rate of earlier stage	veh/h
q_2	Flow rate of platoon	veh/h
q_3	Flow rate of late stage	veh/h
S	Saturation flow rate	veh/h
Intermediate variable		
D_V	Vehicle delay per cycle at adjacent closely spaced intersections	s
d_p	Pedestrian total delay per cycle at closely spaced intersections	s
d_{ij}^v	Average delay of vehicles at entrance lane j under phase i	s
d_{ij}^p	Average pedestrian delay at entrance lane j under phase i	s
d_v^1	The total delay per cycle of nonarterial road	s
D_e	The total delay per cycle of arterial road	s
λ_i	Green time ratio at phase i	—
X	Saturation of intersection	—
k_e^m	Traffic density under scenario m	veh/km
t_c^m	Platoon gathering time under scenario m	s
t_e^m	Dissipation time of vehicles under scenario m	s
d_e^m	Average delay of arterial road under scenario m	s
L_e^m	Maximum queue length under scenario m	m
L_1	Length of the upstream link	m
L_2	Length of the downstream link	m
T_a	The time of vehicle platoon arrive at the downstream intersection	s
Parameter		
m	Scenario number	—
n_m	Dynamic weight factor under scenario m	—
L_{lose}	Signal lost time	s
T	Duration of analysis	h
K	Incremental delay factor	
I	Incremental delay factor	

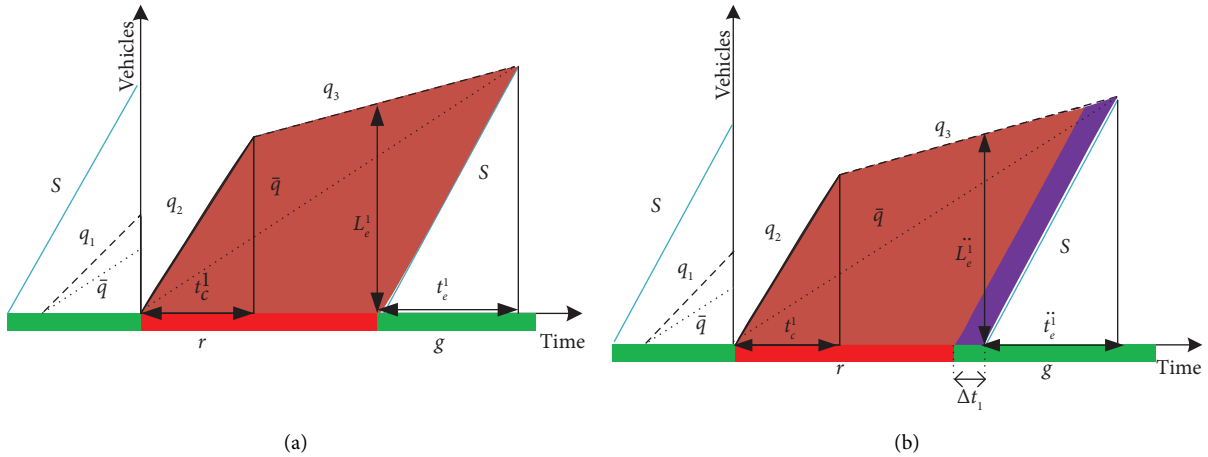

Figure 3: The vehicle platoons reach downstream at the initial red phase. (a) Vehicle delay without the impact of pedestrians. (b) Vehicle delay under the influence of pedestrians.

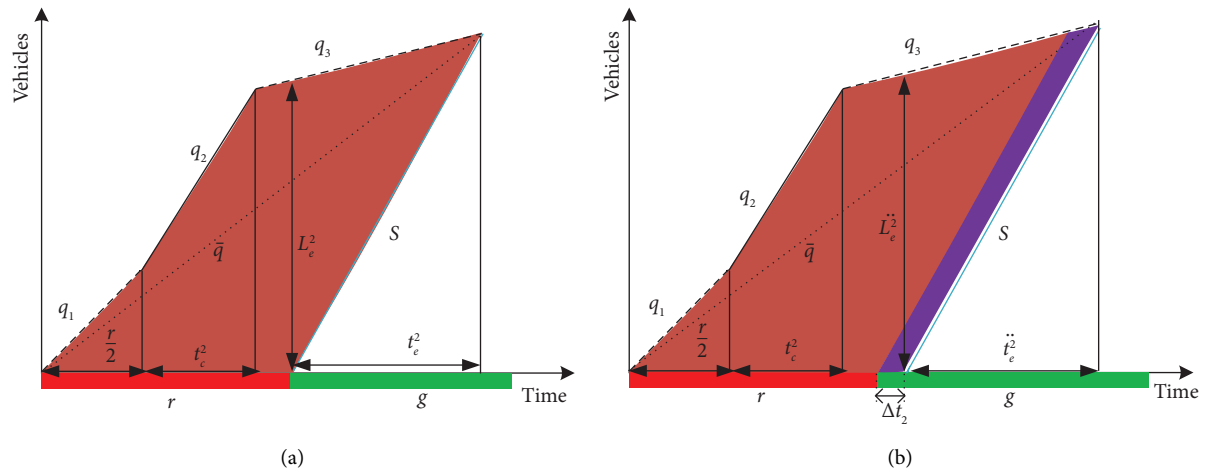

Figure 4: The vehicle platoons reach downstream in the middle of the red phase. (a) Vehicle delay without the impact of pedestrian. (b) Vehicle delay under the influence of pedestrian.

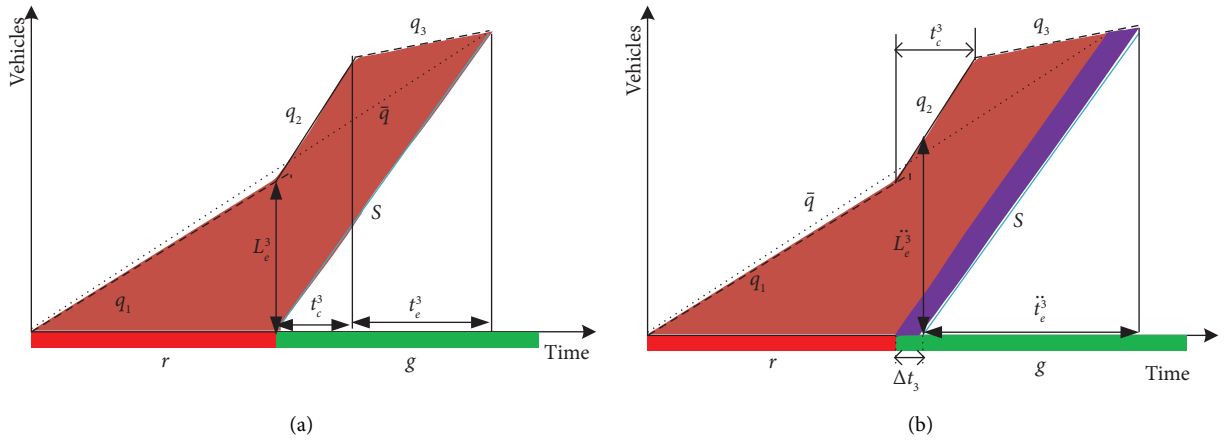

Figure 5: The vehicle platoons reach downstream at the initial green phase. (a) Vehicle delay without the impact of pedestrian. (b) Vehicle delay under the influence of pedestrian.

$$d_e^2 = \int_0^{t_c^2} [(q_1 + q_2)t + (q_1 - q_2)0.5r]\mathrm{d}t + \int_{t_c^2+(r/2)}^{r} \left[(2q_3 - s)t + r(q_1 - q_3 + s) + 2t_c^2(q_2 - q_3)\right]\mathrm{d}t,$$
$$\ddot{d}_e^2 = d_e^2 + \int_r^{r+\Delta t_2+\ddot{t}_e^2} \left[(q_3 + s)t + (q_2 - q_3)t_c^2 - r\left[\frac{1}{2}(q_1 - q_3) - s\right] - s\Delta t_2\right]\mathrm{d}t - \ddot{t}_e^2\left(\ddot{t}_e^2 + r\Delta t_2\right)0.5\overline{q}. \tag{4}$$

Figure 5 shows the platoon arriving at the downstream intersection at the initial green phase. Figure 5(a) shows the cumulation of vehicles without the interference of pedestrians. Figure 5(b) shows the results of pedestrian interference. The shaded area in Figures 5(a) and 5(b) represents the vehicle delay. The corresponding calculation is

$$d_e^3 = \int_0^{r} \left[(q_1 + q_2 + q_3 + s)t + (2q_1 - q_2 - q_3 - s) + (q_2 - q_3)t_c^3\right]\mathrm{d}t,$$
$$\ddot{d}_e^3 = d_e^3 + \int_r^{r+\Delta t_3+\ddot{t}_e^3} \left[(q_3 + s)t + (q_2 - q_3)t_c^3 + (q_1 - q_3 - s)r\right]\mathrm{d}t - \ddot{t}_e^3\left(\ddot{t}_e^3 + r + \Delta t_3\right)0.5\overline{q}. \tag{5}$$

Figure 6 shows the platoon arriving at the downstream intersection in the middle of the green phase. Figure 6(a) shows the cumulative situation without pedestrian interference. Figure 6(b) shows the results of pedestrian interference. The shaded area in Figures 6(a) and 6(b) represent the vehicle delay. The corresponding calculation is as follows:

$$\begin{aligned} d_{\mathrm{e}}^{4} &= \int_{0}^{r+t_{\mathrm{e}}^{4}} [(2q_1 - s)t + sr]\mathrm{d}t, \\ \ddot{d}_{\mathrm{e}}^{4} &= d_{\mathrm{e}}^{4} + \int_{r}^{r+\Delta t_4+\ddot{t}4_{\mathrm{e}}} [(q_1 + s)t - sr]\mathrm{d}t - \ddot{t}_{\mathrm{e}}^{4}\left(\ddot{t}_{\mathrm{e}}^{4} + r + \Delta t_4\right)0.5q_1. \end{aligned} \tag{6}$$

The dynamic weight coefficient is utilized to connect four crucial scene delays to improve the validity of model. The arterial road traffic delay model changes according to the time that the vehicle platoon arrives at the downstream intersection. The corresponding equation is

$$D_{\mathrm{e}} = n_1\left(d_{\mathrm{e}}^{1} + \ddot{d}_{\mathrm{e}}^{1}\right) + n_2\left(d_{\mathrm{e}}^{2} + \ddot{d}_{\mathrm{e}}^{2}\right) + n_3\left(d_{\mathrm{e}}^{3} + \ddot{d}_{\mathrm{e}}^{3}\right) + n_4\left(d_{\mathrm{e}}^{4} + \ddot{d}_{\mathrm{e}}^{4}\right). \tag{7}$$

Figure 7 shows the phases of the platoon arrival time. When the arrival time of the platoon is between the early red phase and the middle of the red phase, the weight coefficients was expressed as follows:

$$r_0 \le T_{\mathrm{a}} \le r_1 \; n_3 = n_4 = 0 \; n_1 = 1 - \frac{2\left(T_{\mathrm{a}} - r_0\right)}{r} \; n_2 = 1 - n_1. \tag{8}$$

When the arrival time of the vehicle platoons is between the middle of the red phase and early green phase period, the weight coefficient can be expressed as follows:

$$r_1 \le T_{\mathrm{a}} \le g_0 \; n_1 = n_4 = 0 \; n_2 = 1 - \frac{2\left(T_{\mathrm{a}} - r_1\right)}{r} \; n_3 = 1 - n_2 \tag{9}$$

When the arrival time of the vehicle platoon is in the period between the initial green phase and the middle green phase, the weight coefficient was expressed as follows:

$$g_0 \le T_{\mathrm{a}} \le g_1 \; n_1 = n_2 = 0 \; n_3 = 1 - \frac{2\left(T_{\mathrm{a}} - g_0\right)}{g} \; n_4 = 1 - n_3. \tag{10}$$

When the arrival time of the platoon is in the period between the middle green phase and the end of the green phase, the weight coefficient is expressed as follows:

$$g_1 \le T_{\mathrm{a}} \le r_0, n_2 = n_3 = 0, n_4 = 1 - \frac{2\left(T_{\mathrm{a}} - g_1\right)}{g}, n_1 = 1 - n_4. \tag{11}$$

3.5. Collaborative Pedestrian-Motor Vehicle Optimization Model

3.5.1. Vehicle Delay Model. The vehicle delay model is the sum of the arterial road traffic delay model and the non-arterial road traffic delay model. The formula is as follows:

$$D_{\mathrm{V}} = d_{\mathrm{v}}^{1} + D_{\mathrm{e}}. \tag{12}$$

3.5.2. Crossing Pedestrian Delay Model. The HCM2010 model is used to calculate the pedestrian delay. The calculation formula is

$$d_{ij}^{\mathrm{p}} = \frac{\left(C - g_{\mathrm{p}}\right)^2}{2c}. \tag{13}$$

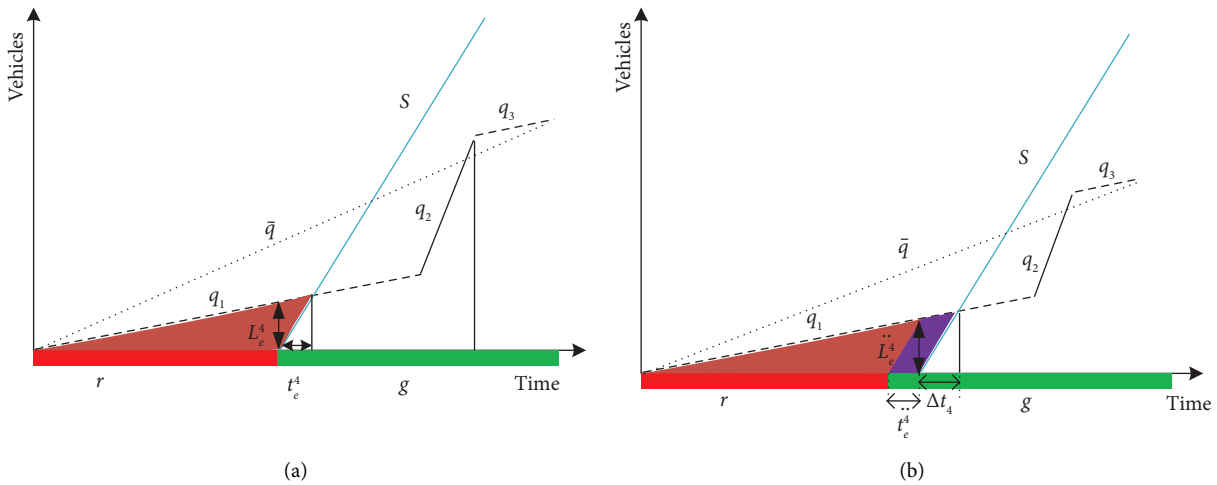

Figure 6: The vehicle platoons reach downstream in the middle of the green phase. (a) Vehicle delay without the impact of pedestrian. (b) Vehicle delay under the influence of pedestrian.

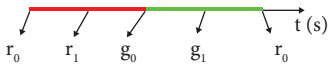

Figure 7: A partition diagram of the vehicle platoon arrival time.

Then, the total delay model of pedestrian crossing is as follows:

$$d_{\mathrm{p}} = \sum_{i} \sum_{j} d_{ij}^{\mathrm{p}} q_{ij}^{\mathrm{p}}. \tag{14}$$

3.5.3. The Objective Optimization. Pedestrians and motor vehicles are simultaneously considered to improve the overall operational efficiency.

$$\min \ D_{\mathrm{v}} + d_{\mathrm{p}}. \tag{15}$$

3.5.4. Constraint Condition. The constraints are set to achieve better performance, including the cycle time constraint, the effective green time constraint, the link length, distance constraint, and the pedestrian crossing time constraint.

(a) Constraint for control variable C: The value of the cycle length constraint is based on the HCM2010 manual. The maximum value cannot exceed the locally accepted maximum cycle length. The minimum value cannot be less than the minimum length required for pedestrians to cross the street at the intersection, depending on the width of the street.

$$\begin{aligned} &C_{\min} \le C \le C_{\max}, \\ &C = \sum_{i}^{m} g_i + L_{\mathrm{lose}}, \\ &C_{\mathrm{A}} = C_{\mathrm{B}}. \end{aligned} \tag{16}$$

(b) Constraint for control variable g: The effective time of the green phase should not be too long to make pedestrians wait too long. The minimum time of the green phase should ensure that the vehicles are able to leave and the pedestrians are able to cross the street. The constraint of green phase is as follows:

$$\begin{aligned} &g_{\min} \le g_i \le g_{\max}, \\ &g_{\min} = \frac{c q_{ij}}{S_i}. \end{aligned} \tag{17}$$

(c) Constraint for the state variable λ: To improve the efficiency of green phase, a minimum green ratio is set. The following relation is shown:

$$\begin{aligned} &\lambda_i = \frac{g_i}{C}, \\ &\lambda_i \ge \lambda_{\min}. \end{aligned} \tag{18}$$

(d) Constraint for the state variable L: Queue overflow sections as the connection lanes will directly lead to internal adjacent closely spaced intersections locked. The maximum queue length should not exceed the connection section length. It is noted that the length of the intersection line section is different as the platoon arrived in time and changed. Hence, the maximum queue length of all the scenarios is calculated firstly. Then, the dynamic weight coefficient is used to connect the maximum queue length in each scenario, and the calculation model of the maximum queue length at the link section is obtained. The formula is as follows:

$$
\begin{aligned}
L_e^1 &= \left[q_3 r + (q_2 - q_3)t_c^1\right]k_e^1,\\
L_e^2 &= \left[\frac{1}{2}r(q_1 + q_3) + t_c^2(q_2 - q_3)\right]k_e^2,\\
L_e^3 &= q_1 r k_e^3,\\
L_e^4 &= q_1 r k_e^4,\\
\ddot{L}_e^1 &= \left[(r + \Delta t_1)q_3 + (q_2 - q_3)t_c^1\right]k_e^1,\\
\ddot{L}_e^2 &= \left[\frac{1}{2}(r + \Delta t_2)(q_1 + q_3) + t_c^2(q_2 - q_3)\right]k_e^2,\\
\ddot{L}_e^3 &= q_1(r + \Delta t_3)k_e^3,\\
\ddot{L}_e^4 &= q_1(r + \Delta t_4)k_e^4,\\
L_e &= n_1\left(L_e^1 + \ddot{L}_e^1\right) + n_2\left(L_e^2 + \ddot{L}_e^2\right)\\
&\quad + n_3\left(L_e^3 + \ddot{L}_e^3\right) + n_4\left(L_e^4 + \ddot{L}_e^4\right),\\
L_e &\le \max\{L_1, L_2\}.
\end{aligned}
\tag{19}
$$

3.6. Solving Algorithm. Genetic algorithm (GA) is a parameter random search algorithm, which is based on bionic principles to simulate biological genetics and natural selection laws. The algorithm can search quickly within the solution space according to the algorithm flow. The essence of GA is an iterative algorithm. It will generate a certain number of populations according to a certain coding mode, and the population is randomly generated. Then, it was evaluated by the fitness function. Then, the corresponding selection operation, crossover operation, and mutation operation are carried out on the population. Finally, the optimal parameter solution set is obtained after several iterations. Figure 8 shows the flow chart of solving algorithm. The steps of GA are as follows:

Step 1. The genetic algorithm parameters such as termination condition, coding mode, population number, crossover probability, and mutation probability were determined, and the iteration counter was set to 0.

Step 2. The fitness function value of the generated population was calculated.

Step 3. According to the specific selection strategy, some individuals were selected from the population based on the fitness function value of the population.

Step 4. The genetic characteristics of the biological cell division were simulated. The next generation is replicated from the excellent population characteristics of the previous generation.

Step 5. Groups are operated by crossover operators.

Step 6. Determining the probability of mutating a population to create a new population.

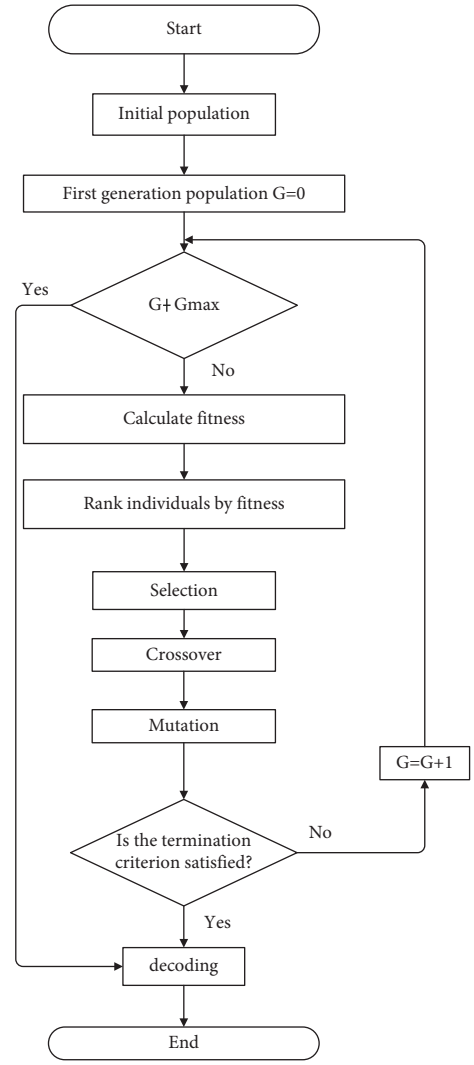

Figure 8: Genetic algorithm flowchart.

Step 7. Judge the convergence condition of the algorithm. If the condition is satisfied, the algorithm converges. Otherwise, continue the algorithm.

3.7. Case Validation. This study selected the adjacent closely spaced intersections in Suihua City, Heilongjiang Province, China. The intersection is a significant location in an urban area. The congestion of the intersection is quite severe. The current signal scheme is based on the HCM2010 isolated intersection timing without consideration of pedestrians using synchro calculations. The channelization and signal control scheme of the intersection are shown in Figures 9 and 10.

The data of traffic flow and pedestrian are from 6:45 a.m. to 7:45 a.m. on November 17, 2019, as shown in Table 3.

3.8. Case Optimization. The optimization of signal control is conducted to verify the reliability of the optimization model. The MATLAB is used to write the genetic algorithm target program. The models are optimized for four different

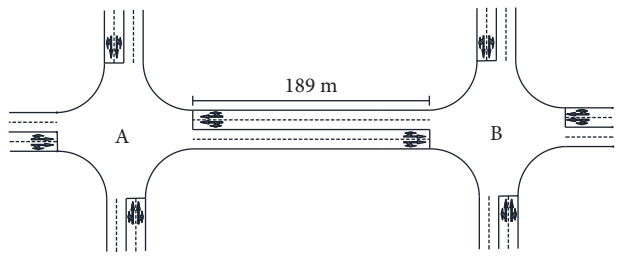

Figure 9: Channelized diagram of the two intersections.

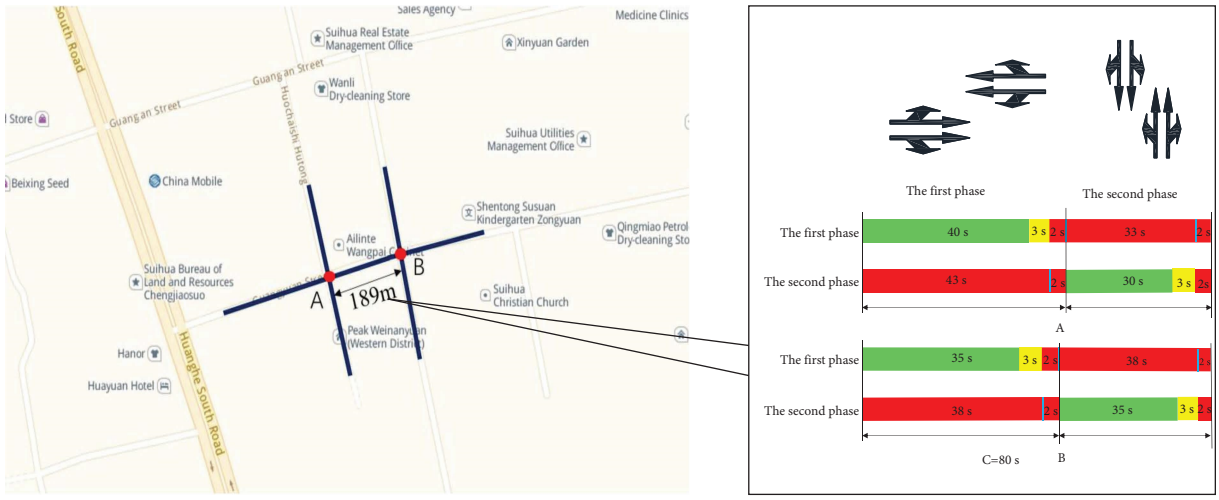

Figure 10: Signal scheme of the intersection.

Table 3: Traffic flow at the intersections.

Intersection name	South entrance			North entrance			East entrance			West entrance		
A (veh/h)	Left	Straight	Right	Left	Straight	Right	Left	Straight	Right	Left	Straight	Right
	97	632	145	89	736	210	117	1028	218	108	1126	178
Pedestrian flow (ped/h)		517			481			477			396	
B (veh/h)	Left	Straight	Right	Left	Straight	Right	Left	Straight	Right	Left	Straight	Right
	76	572	108	127	606	158	112	1276	84	142	984	100
Pedestrian flow (ped/h)		524			467			289			341	

scenarios where the platoon arrives at the downstream intersection at the moment of early red, midred, early green, and midgreen. Genetic algorithm convergence graphs are shown in Figure 11, and the optimized schemes are summarized in Table 4.

3.9. Comparative Analysis of Optimization Effects. In order to verify the effectiveness of the model, the signal timing in four scenarios is optimized. Delays for vehicles and pedestrians were calculated and compared with the isolated intersection signal timing. The current signal control scheme and traditional signal timing control for isolated intersections are obtained by establishing the delay model using MATLAB.

As shown in Figure 12, it was found that the total vehicle delay of the system under this collaborative pedestrian-vehicle scheme is relatively low. These conditions are the arrival of the vehicle platoon early in the red phase, in the middle of the red phase, early in the green phase, and in the middle of the green phase. Based on the proposed model, the total delay has decreased by 13%, 22.6%, 24.8%, and 31.1%, respectively, for these periods.

It can also be concluded from Figure 13 that the total delay of the pedestrians is relatively low. Under the collaborative pedestrian-vehicle optimization method, the total pedestrian delay has decreased by 11%, 22%, 31.6%, and 37% for these four periods, respectively. The signals vary with time the platoon arrives. Compared with the signal timing control, the collaborative pedestrian-motor vehicle control shows significant advantage, and the optimization result reflects the rationality of the model.

A comparison of the traditional signal timing control for isolated intersection with the collaborative optimization model is shown in Figure 14. The statistics show that the total vehicle delay of the proposed model is reduced by 4%, 13.8%, 17.1%, and 25.9%, respectively.

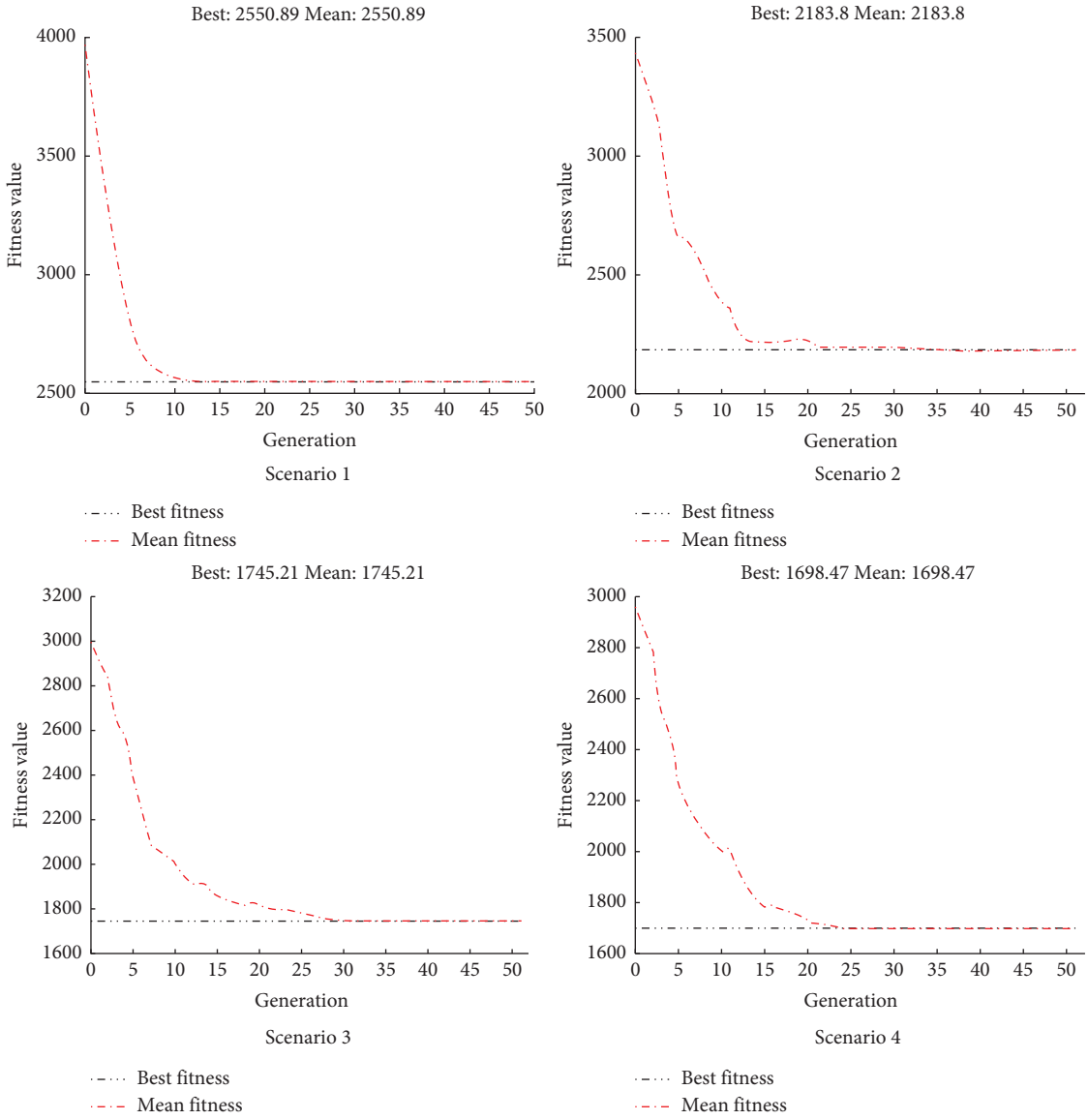

Figure 11: Genetic algorithm convergence graphs.

Table 4: Collaborative optimization scheme for four scenarios.

Intersection	The first phase (s)	The second phase (s)	Cycle (s)
Scenario 1			
A	38	26	71
B	39	25	
Scenario 2			
A	37	22	66
B	36	23	
Scenario 3			
A	29	27	63
B	29	27	
Scenario 4			
A	29	26	62
B	29	26	

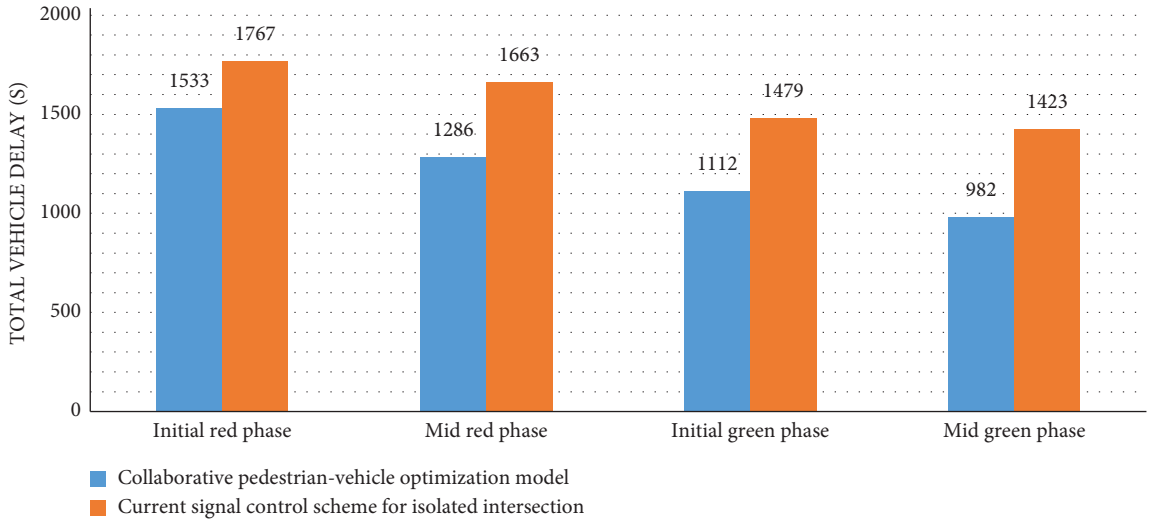

Figure 12: Comparison chart with current vehicle delays.

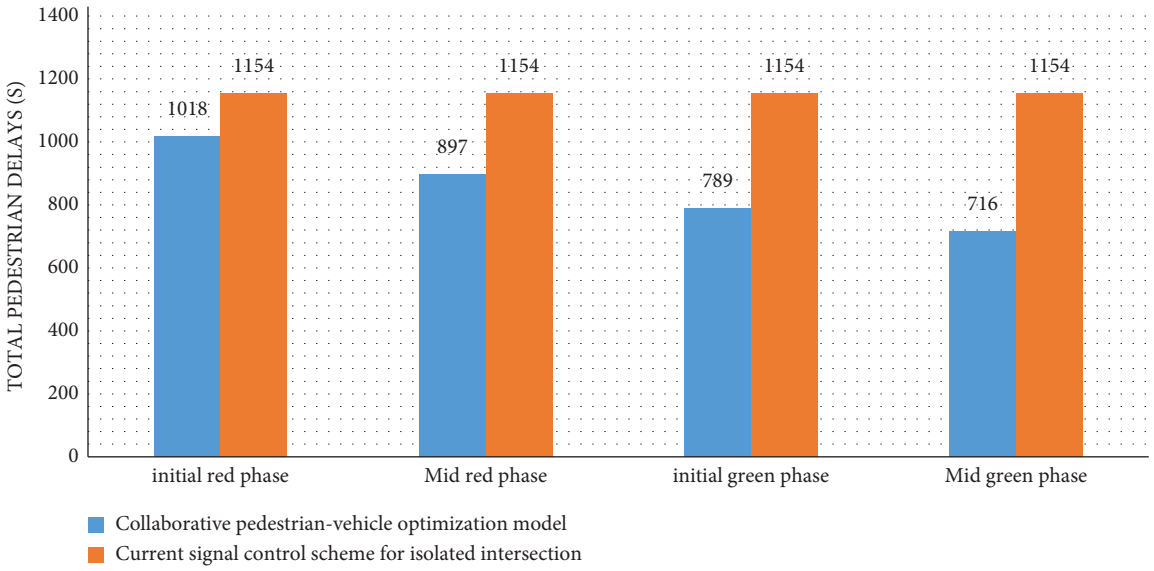

Figure 13: Pedestrian delay comparison chart with the current situation.

It can be seen from Figure 15 that the total pedestrian delay of the system under the collaborative pedestrian-motor vehicle optimization method for adjacent closely spaced intersections is lower than that under the traditional isolated intersections timing control. The four periods have decreased by 3%, 15%, 25%, and 31%, respectively. Compared with the conventional isolated intersections timing optimization method, the collaborative optimization model has significant advantages.

Through comparative analysis, we found that the optimization effect was not apparent when the vehicle platoons arrived at the initial red phase. In the original timing scheme, the delay of vehicles is the highest when the vehicle platoons arrive at the initial red phase, which will have an impact on the stability of the entire adjacent closely spaced intersections system. At this time, the optimized signal timing increases the green time ratio of the arterial traffic and reduces the delay of vehicles and pedestrians in the adjacent closely spaced intersections system.

When the vehicle platoons reach the downstream intersection in the green phase, the green time ratio of the optimized signal arterial traffic and the nonarterial traffic is similar. It reflects the character of the optimization model that the signal timing is adjusted according to the time when the vehicle platoons arrive at the downstream intersection. The optimization effect is also pronounced.

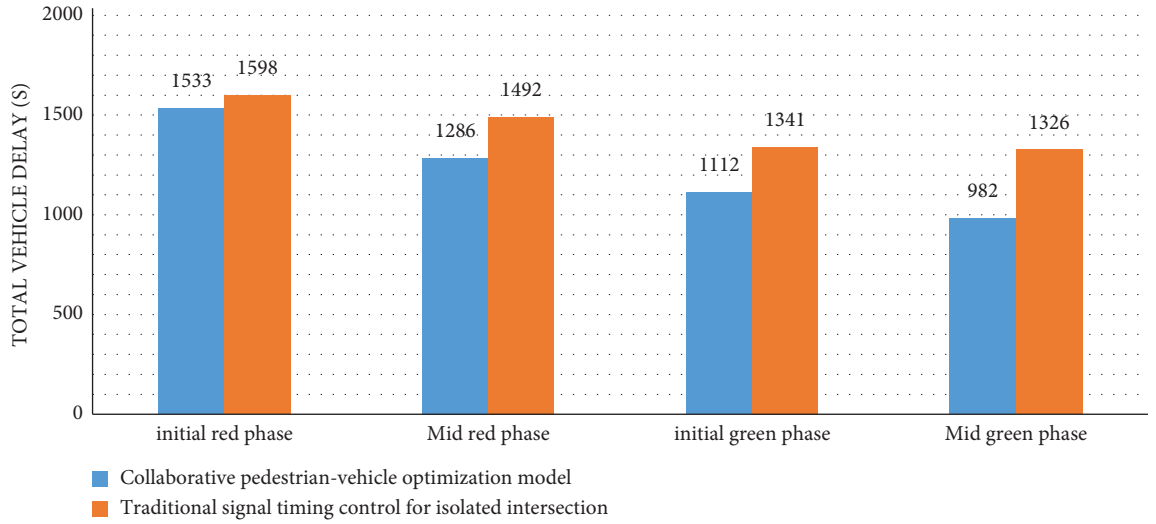

Figure 14: Comparison of vehicle delays with traditional isolated intersections' optimization schemes.

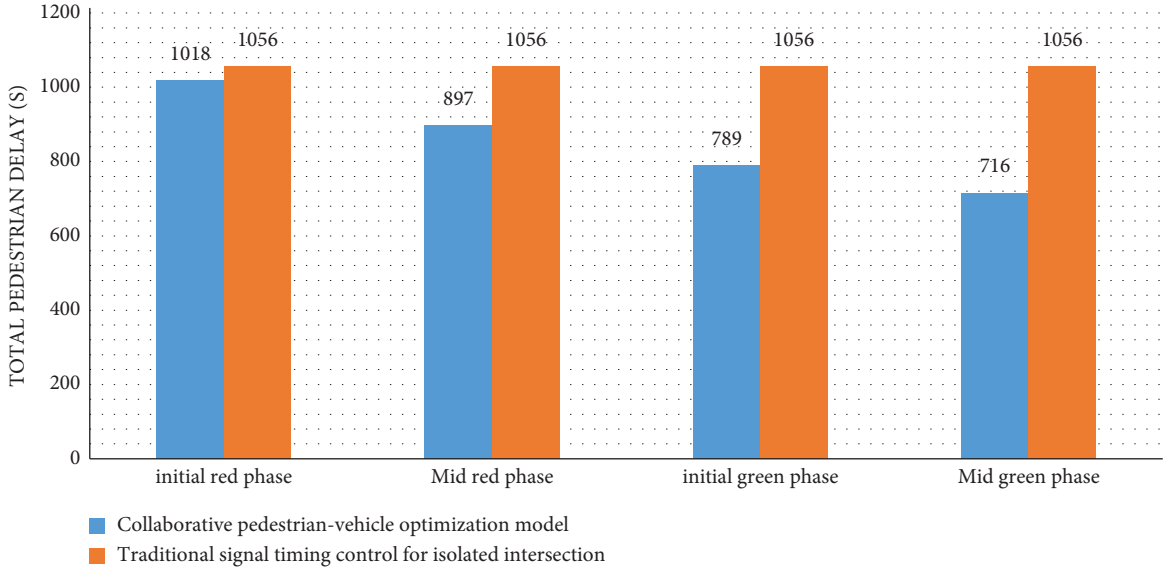

Figure 15: Pedestrian delay comparison chart with traditional isolated intersections' optimization scheme.

4. Conclusion and Future Work

In this paper, a new signal control optimization method for pedestrians and vehicles at adjacent closely spaced intersections has been proposed. The optimization and operations research has created a simulation platform. The experimental results demonstrate the effectiveness of this method. The conclusions from this study are as follows:

(a) By including the demand of pedestrian crossing, several signal control strategies have been proposed. Corresponding delay models are established according to time when a motorcade arrives. A proposed scene delay is linked by dynamic weight coefficients. A signal optimization is achieved. This reduces the delay between vehicles and pedestrians. Pedestrians and motor vehicles spend shorter time at the intersections which results in improved safety.

(b) We applied this method to a real case to verify its effectiveness. The model is compared with the current control scheme for isolated intersections and a traditional isolated intersections timing control. The optimization efficiency of this new model is obvious.

For future research work, fuel consumption, carbon emissions, and other parameters should be considered to refine this method.

Data Availability

All the data used to support the findings of this study are included within the article.

Conflicts of Interest

The authors declare that they have no conflicts of interest.

Acknowledgments

The authors acknowledge the research grants from the National Natural Science Foundation of China under grant no. 52102398 and Science & Technology Commission of Shanghai Municipality under grant no. 23692107600.

References

[1] L. Wang, K. Wang, J. Zhang, D. Zhang, X. Wu, and L. Zhang, "Multiple objective-oriented land supply for sustainable transportation: a perspective from industrial dependence, dominance and restrictions of 127 cities in the Yangtze River Economic Belt of China," *Land Use Policy*, vol. 99, Article ID 105069, 2020.

[2] P. Fernandes, M. C. Coelho, and N. M. Rouphail, "Assessing the impact of closely-spaced intersections on traffic operations and pollutant emissions on a corridor level," *Transportation Research Part D: Transport and Environment*, vol. 54, pp. 304–320, 2017.

[3] A. Zhou, S. Peeta, M. Yang, and J. Wang, "Cooperative signal-free intersection control using virtual platooning and traffic flow regulation," *Transportation Research Part C: Emerging Technologies*, vol. 138, p. 103610, 2022.

[4] Z. Zhang and Z. Tian, "Calculation of additional lost green time at closely spaced intersections," *International Journal of Transportation Science and Technology*, vol. 2, no. 2, pp. 109–122, 2013.

[5] L. Chen, J. Li, Y. Li, and J. Yao, "Comprehensive evaluation of operational efficiency of intersections in arterial considering pedestrians yield rule," *Journal of Advanced Transportation*, vol. 2022, Article ID 6871290, 25 pages, 2022.

[6] F. Ahmed and Y. E. Hawas, "An integrated real-time traffic signal system for transit signal priority, incident detection and congestion management," *Transportation Research Part C: Emerging Technologies*, vol. 60, pp. 52–76, 2015.

[7] B. Li, "A model of pedestrians' intended waiting times for street crossings at signalized intersections," *Transportation Research Part B: Methodological*, vol. 51, pp. 17–28, 2013.

[8] A. M. Roshandeh, Z. Li, S. Zhang, H. S. Levinson, and X. Lu, "Vehicle and pedestrian safety impacts of signal timing optimization in a dense urban street network," *Journal of Traffic and Transportation Engineering*, vol. 3, no. 1, pp. 16–27, 2016.

[9] C. Yu, W. Ma, K. Han, and X. Yang, "Optimization of vehicle and pedestrian signals at isolated intersections," *Transportation Research Part B: Methodological*, vol. 98, pp. 135–153, 2017.

[10] W. Li, H. Zhang, Z. Huang, and C. Li, "Human-vehicle intersection traffic lights timing optimization research," *Journal of Advanced Transportation*, vol. 2022, Article ID 5549454, 9 pages, 2022.

[11] X. Liu, H. Yuan, J. Hu, and X. Jiao, "Single-point adaptive control method for urban mixed traffic flow," *Journal of Advanced Transportation*, vol. 2020, Article ID 8827824, 7 pages, 2020.

[12] J. Zhao, W. Ma, and P. Li, "Optimal design of midblock crosswalk to achieve trade-off between vehicles and pedestrians," *Journal of Transportation Engineering, Part A: Systems*, vol. 143, no. 1, 2017.

[13] Y. Xinwu, W. Qiaohui, X. Huibin, and X. Xiaoyan, "A coordinated signal control method for arterial road of adjacent intersections based on the improved genetic algorithm," *Optik*, vol. 127, no. 16, pp. 6625–6640, 2016.

[14] Y. L. Gu and C. F. Shao, "Study on coordinated control of traffic signal for adjacent intersections," *Advanced Materials Research*, vol. 433-440, pp. 4765–4770, 2012.

[15] Y. Zou, R. Liu, Y. Li, Y. Ma, and G. Wang, "Signal adaptive cooperative control of two adjacent traffic intersections using a two-stage algorithm," *Expert Systems with Applications*, vol. 174, p. 114746, 2021.

[16] M. Zhang, L. Jia, and W. Zhu, "A cell-based robust optimal coordinated control on urban arterial road," *Journal of Control Theory and Applications*, vol. 10, no. 4, pp. 543–548, 2012.

[17] R. Van Houten, R. A. Retting, C. M. Farmer, and J. Van Houten, "Field evaluation of a leading pedestrian interval signal phase at three urban intersections," *Transportation Research Record*, vol. 1734, no. 1, pp. 86–92, 2000.

[18] E. Goughnour, D. Carter, C. Lyon et al., "Evaluation of protected left-turn phasing and leading pedestrian intervals effects on pedestrian safety," *Transportation Research Record: Journal of the Transportation Research Board*, vol. 2675, no. 11, pp. 1219–1228, 2021.

[19] P. G. Furth and R. M. Saeidi Razavi, "Leading through intervals versus leading pedestrian intervals: more protection with less capacity impact," *Transportation Research Record*, vol. 2673, no. 9, pp. 152–164, 2019.

[20] S. Saneinejad and J. Lo, "Leading pedestrian interval: assessment and implementation guidelines," *Transportation Research Record: Journal of the Transportation Research Board*, vol. 2519, no. 1, pp. 85–94, 2019.

[21] D. Zhu and N. N. Sze, "Propensities of red light running of pedestrians at the two-stage crossings with split pedestrian signal phases," *Accident Analysis & Prevention*, vol. 151, Article ID 105958, 2021.

[22] P. Gårder, "Pedestrian safety at traffic signals: a study carried out with the help of a traffic conflicts technique," *Accident Analysis & Prevention*, vol. 21, no. 5, pp. 435–444, 1989.

[23] K. E. M. A. K. Bechtel and D. R. Ragland, "Pedestrian scramble signal in chinatown neighborhood of oakland, california," *Transportation Research Record*, vol. 1878, pp. 19–26, 2004.

[24] J. Wang, C. Yang, and J. Zhao, "Conditions for setting exclusive pedestrian phases at two-phase signalized intersections considering pedestrian-vehicle interaction," *Journal of Advanced Transportation*, vol. 2021, Article ID 8546403, 14 pages, 2021.

[25] D. Juozevičiūtė and V. Grigonis, "Evaluation of exclusive pedestrian phase safety performance at one-level signalized intersections in vilnius," *Sustainability*, vol. 14, no. 13, p. 7894, 2022.

[26] F. Chen, L. Wang, B. Jiang, and C. Wen, "An arterial traffic signal control system based on a novel intersections model and improved hill climbing algorithm," *Cognitive Computation*, vol. 7, no. 4, pp. 464–476, 2015.